PNAS

Supporting Information for

Molecular basis of signal transduction mediated by the human GIPR splice variants

Fenghui Zhao[a,b,1], Kaini Hang[c,d,1], Qingtong Zhou[e,f,1], Lijun Shao[c,d], Hao Li[f], Wenzhuo Li[a,b], Shi Lin[f], Antao Dai[a,b], Xiaoqing Cai[a,b], Yanyun Liu[a,b,g], Yingna Xu[e], Wenbo Feng[e], Dehua Yang[a,b,f,g,*], Ming-Wei Wang[e,f,h,i,*]

[a]The National Center for Drug Screening, Shanghai Institute of Materia Medica, Chinese Academy of Sciences, Shanghai 201203, China; [b]State Key Laboratory of Chemical Biology, Shanghai Institute of Materia Medica, Chinese Academy of Sciences, Shanghai 201203, China; [c]iHuman Institute, ShanghaiTech University, Shanghai 201210, China; [d]School of Life Science and Technology, ShanghaiTech University, Shanghai 201210, China; [e]Department of Pharmacology, School of Basic Medical Sciences, Fudan University, Shanghai 200032, China; [f]Research Center for Deepsea Bioresources, Sanya, Hainan 572025, China; [g]School of Chinese Materia Medica, Nanjing University of Chinese Medicine, Nanjing 210023, China; [h]Department of Chemistry, School of Science, The University of Tokyo, Tokyo 113-0033, Japan; [i]School of Pharmacy, Hainan Medical University, Haikou, 570228, China.

[1]F.Z., K.H. and Q.Z. contributed equally to this work.

*To whom correspondence may be addressed. Email: Dehua Yang (dhyang@simm.ac.cn) or Ming-Wei Wang (mwwang@simm.ac.cn)

This PDF file includes:

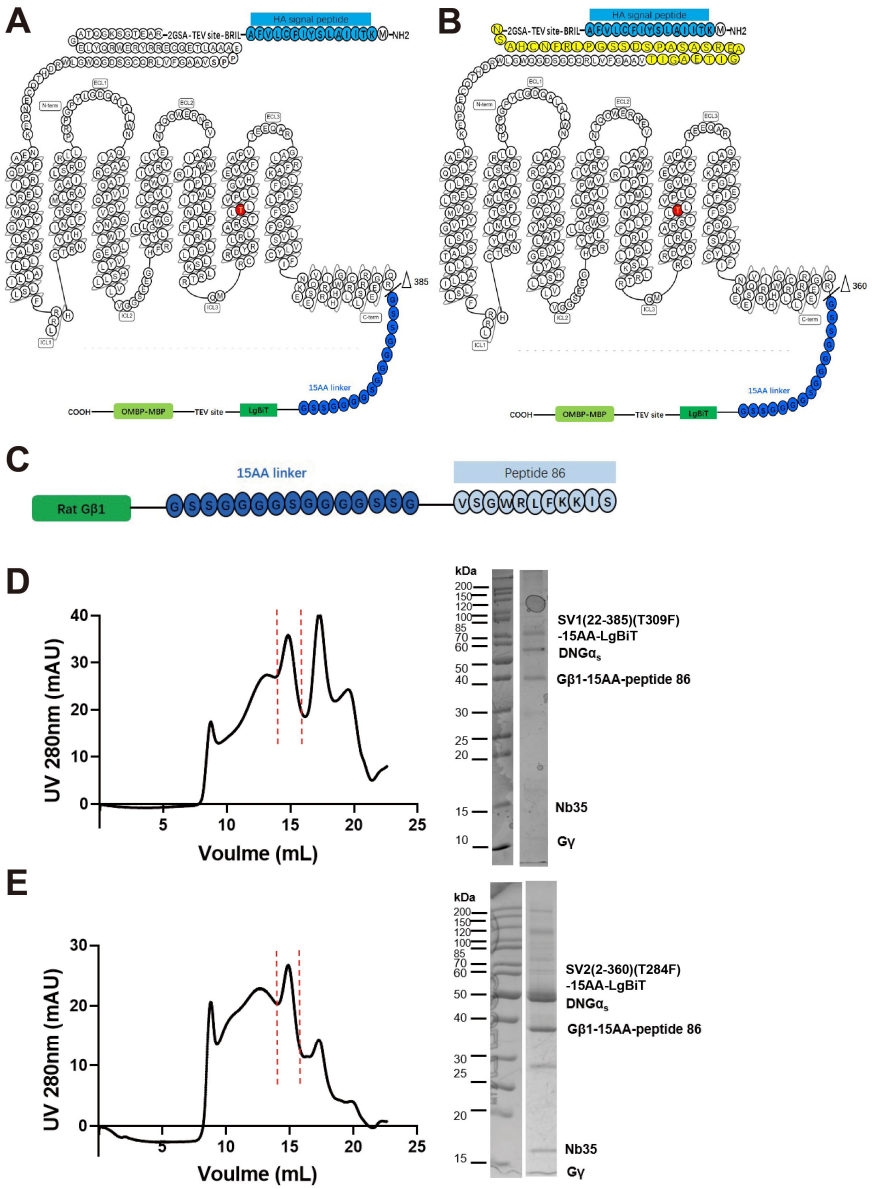

Figure S1. Purification and characterization of the SV1–G_s–Nb35 and SV2–G_s–Nb35 complexes. (***A***) Schematic of HA-BRIL-TEV-2GSA-SV1(22-385)(T309F)-15AA-LgBiT-TEV-OMBP-MBP construct used in cryo-EM study. (***B***) HA-BRIL-TEV-2GSA-SV2(2-360)(T284F)-15AA-LgBiT-TEV-OMBP-MBP construct used in cryo-EM study. The new sequence of SV2 was highlighted in yellow. The HA signal peptide was highlighted in blue. SV1 and SV2 were truncated at R385 and R360, respectively, followed by a 15-amino acid linker (15AA, dark blue) and LgBiT (green). The C terminus was modified with a TEV protease site and an OMBP-MBP (light green) tag. The mutation site at $T^{6.44b}F$ (T309F at SV1 or T284F at SV2) was highlighted in red. (***C***) Gβ1 constructs used for structure determination. Rat Gβ1 (dark green) was attached to peptide 86 (light blue) with a 15AA linker (dark blue) between them. (***D***) Size-exclusion chromatography results of the SV1(22-385)(T309F)–G_s–Nb35 (red line) complex on Superose 6 Increase 10/300GL (left panel) and the SDS-PAGE results of the complexes (right panel). (***E***) Size-exclusion chromatography results of the SV2(2-360)(T284F)–G_s–Nb35 (red line) complex on Superose 6 Increase 10/300GL (left panel) and the SDS-PAGE results of the complexes (right panel).

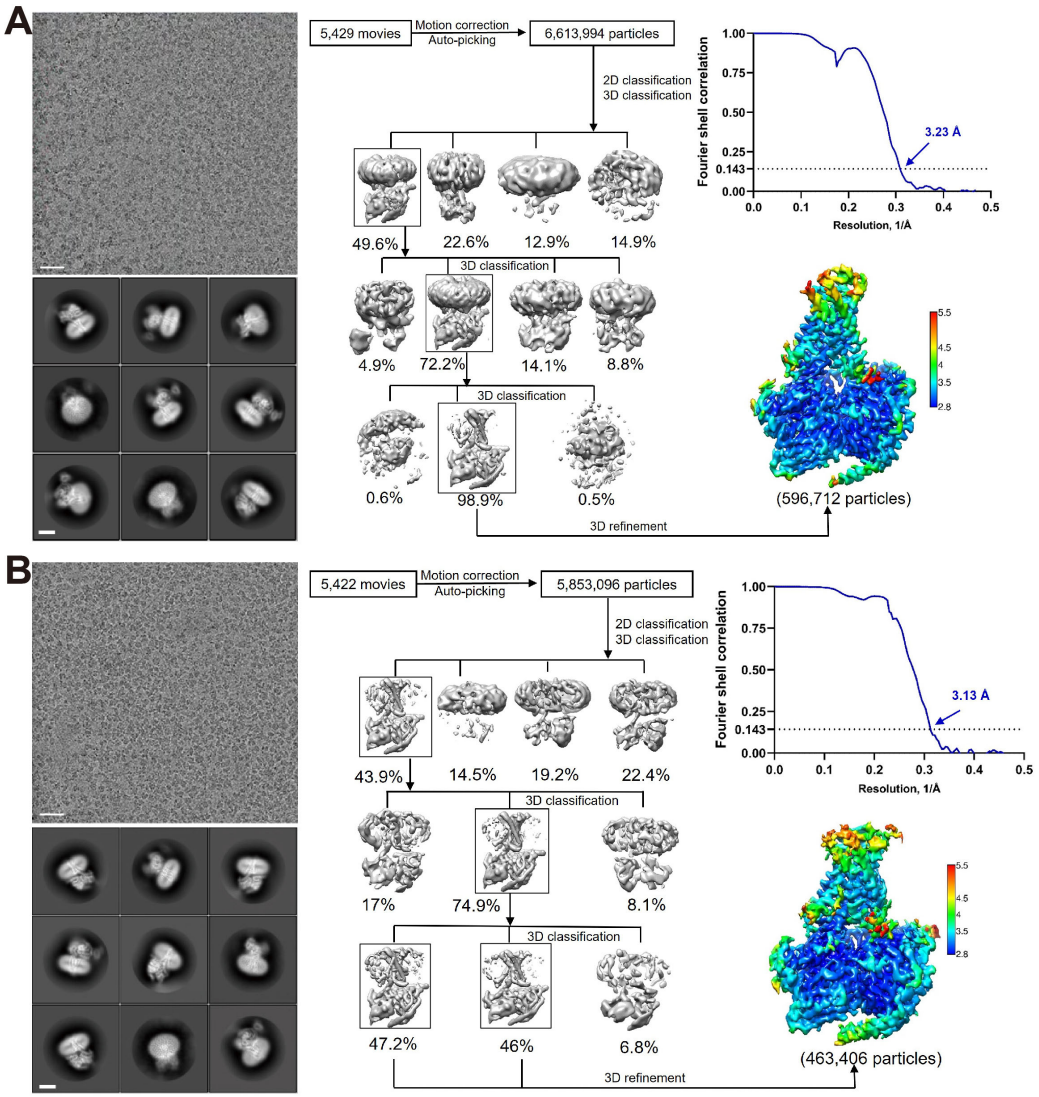

Figure S2. Cryo-EM data processing and validation. (*A*) SV1–G_s complex: representative cryo-EM micrograph (scale bar: 40 nm) (top left panel) and two-dimensional (2D) class averages (scale bar: 5 nm) (bottom left panel). Middle panel, flow chart of cryo-EM data processing. Bottom right panel, local resolution distribution map of the SV1–G_s complex. Top right panel, gold-standard Fourier shell correlation (FSC) curves of overall refined receptor. **(*B*)** SV2–G_s complex: representative cryo-EM micrograph (scale bar: 40 nm) (top left panel) and 2D class averages (scale bar: 5 nm) (bottom left panel). Middle panel, flow chart of cryo-EM data processing. Bottom right panel, local resolution distribution map of the SV2–G_s complex. Top right panel, gold-standard FSC curves of overall refined receptor.

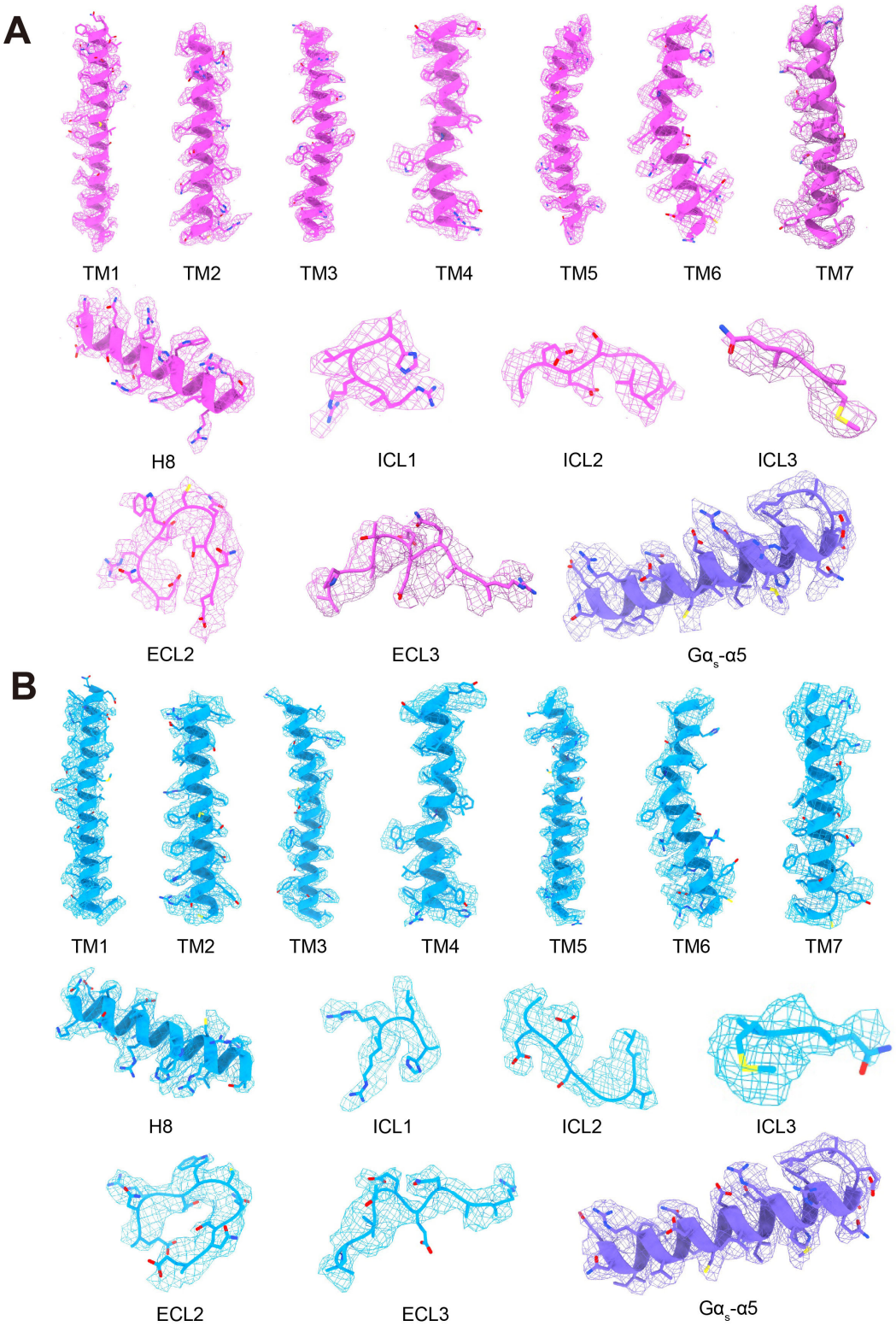

Figure S3. Near-atomic resolution model of the complexes in the cryo-EM density maps. **(*A*)** EM density map and model of the SV1–G_s complex are shown for all seven-transmembrane α-helices (7TMs), helix 8 (H8), intracellular loops (ICLs), extracellular loops 2 (ECL2) and 3 (ECL3) of SV1, the α5-helix of the $G\alpha_s$ Ras-like domain. **(*B*)** EM density map and model of the SV2–G_s complex are shown for all 7TMs, H8, ICLs, ECL2 and ECL3 of SV2, the α5-helix of the $G\alpha_s$ Ras-like domain.

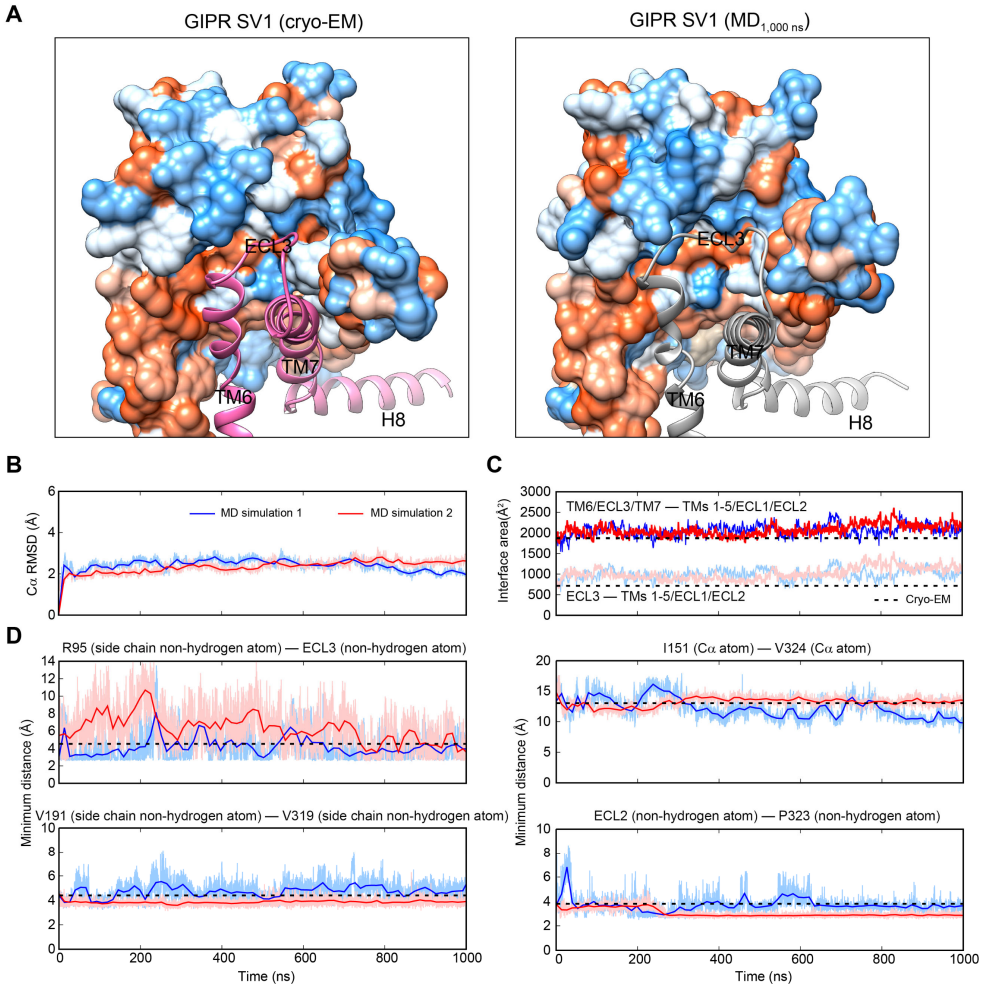

Figure S4. Molecular dynamics (MD) simulation of GIPR SV1. (***A***) Comparison of GIPR SV1 conformation between the cryo-EM structure (hot pink) and the final MD simulation snapshot (gray). To restrain the GIPR SV1 in its G protein complex conformation, harmonic restraints were placed on all Cα atoms within 5 Å of the G protein binding interface during the MD simulation. TMs 1-5/ECL1/ECL2 (residues 88-292) are shown in surface representation and colored in dodger blue for the most hydrophilic region and orange red for the most hydrophobic region, respectively. TM6-ECL3-TM7-H8 are shown as cartoon to highlight the inward folded conformation of ECL3. (***B***) Root mean square deviation (RMSD) of Cα positions of GIPR SV1 during two independent MD simulations, where all snapshots were superimposed on the cryo-EM structure of GIPR SV1 using the Cα atoms. (***C***) Interface area between TMs 1-5/ECL1/ECL2 (residues 88-292) and extracellular halves of TM6/ECL3/TM7 (residues 310-347, dark line) or ECL3 (residues 318-331, light line) during MD simulation, calculated using freeSASA. (***D***) Representative minimum distances between the non-hydrogen atoms of ECL3 and the surrounding pocket residues: top left, R95 (side chain)–ECL3; top right, I151 (Cα)–V324 (Cα); bottom left, V191 (side chain)–V319 (side chain); bottom right, ECL2–P323. The thick and thin traces represent moving averages and original, unsmoothed values, respectively.

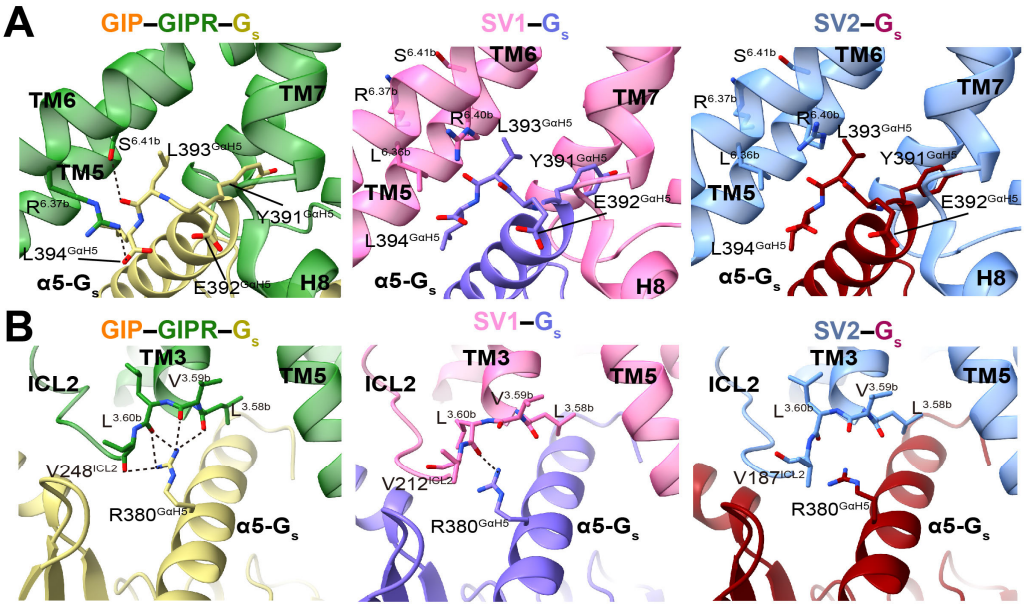

Figure S5. Structural comparison of G protein coupling among GIPR, SV1 and SV2. (***A***) Interaction differences between receptors (GIPR, SV1 and SV2) and the C terminus of $G\alpha_s$. The receptors and G protein are colored as labeled. (***B***) Polar interactions between ICL2 and $G\alpha_s$ for GIPR, SV1 and SV2. The receptors and G proteins are colored as labeled. Polar interactions are shown as black dashed lines.

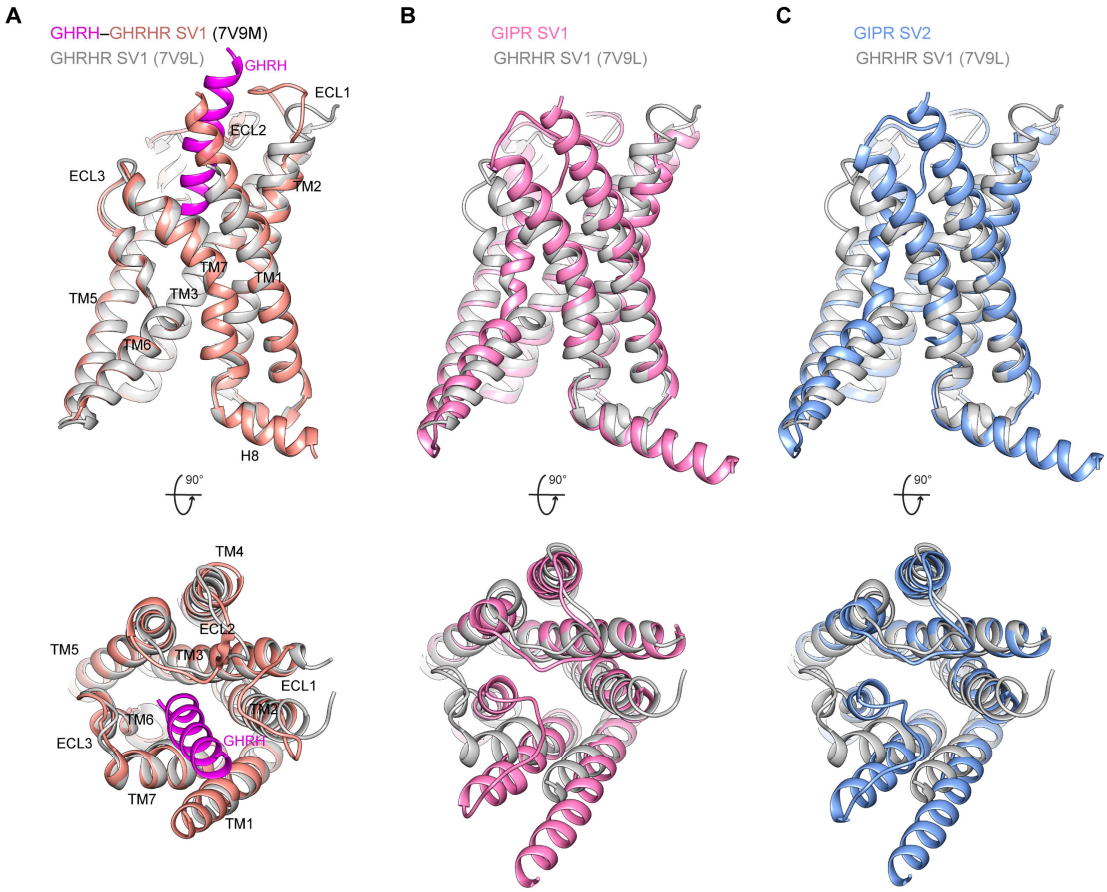

Figure S6. Structural comparison among GHRHR SV1, GIPR SV1 and SV2. The G_s-coupled structures of GHRH-bound GHRHR SV1 (PDB code: 7V9M) and peptide-free GHRHR SV1 (PDB code: 7V9L) are superimposed on the GIPR SV1 or GIPR SV2 structure using the Cα carbons of the TMD residues. Receptor ECD and G protein are omitted for clarity.

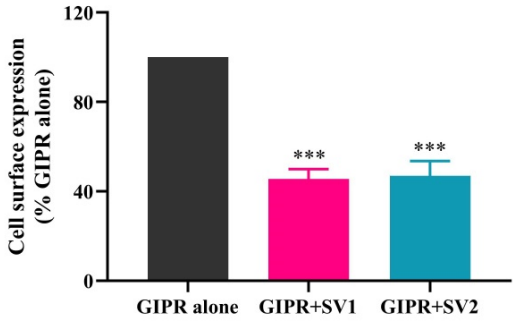

Receptor	Cell surface expression (% GIPR alone)
GIPR alone	100.00
GIPR + SV1	45.52 ± 4.46***
GIPR + SV2	46.90 ± 6.68***

Figure S7. Effects of GIPR splice variants (SVs) on cell surface expression of WT GIPR. The left panel shows the receptor cell surface expression levels, and the right panel shows the quantification. Cells were co-transfected with GIPR and each SV at a ratio of 1:3. Data shown are means ± SEM of four independent experiments (n=4). Data were normalized to the GIPR alone group. One-way ANOVA was used to determine statistical difference (***P<0.001).

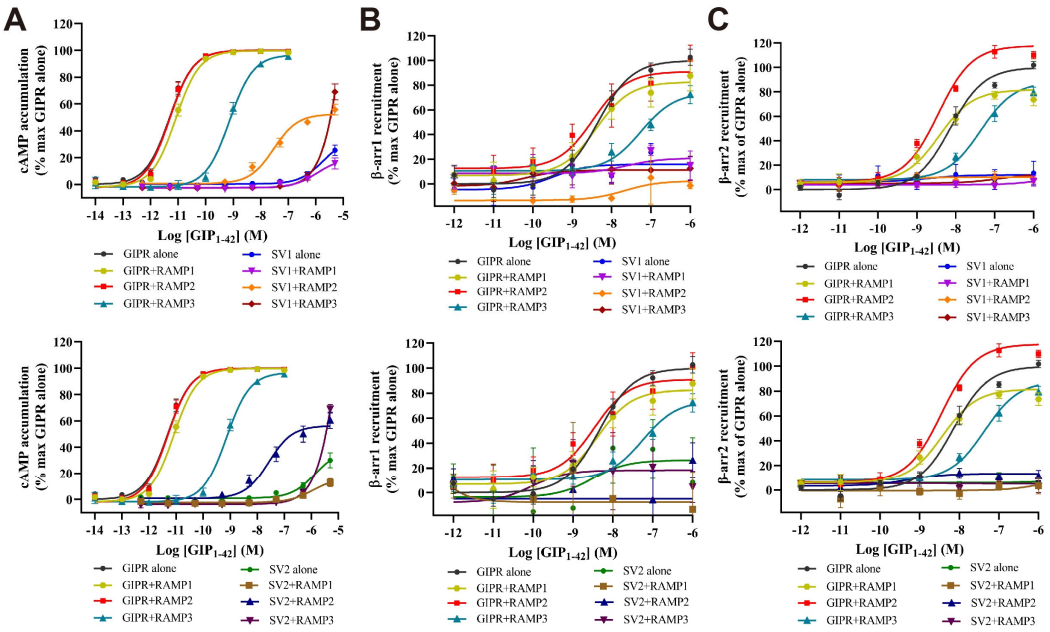

Figure S8. Signaling profiles of GIP_{1-42} at GIPR, SV1 or SV2 when coexpressed with RAMPs. (***A***) cAMP accumulation induced by GIP_{1-42} at GIPR, SV1 (top) or SV2 (bottom) when coexpressed with RAMPs. The assay was performed in HEK293T cells transiently transfected with constructs of GIPR, SV1 or SV2 with or without individual RAMPs for cAMP accumulation assay. (***B*** and ***C***) β-arrestin 1/2 recruitment induced by GIP_{1-42} at GIPR, SV1 (top) or SV2 (bottom) when coexpressed with or without individual RAMPs. For β-arrestin 1/2 recruitment assay, HEK293T cells were transiently transfected either with GIPR-Rluc8, GRK5 and Venus-β-arrestin 1/2 (β-arr1 and β-arr2) coexpressed with or without individual RAMPs, or with SV1/2-Rluc8, GRK5 and Venus-β-arrestin 1/2 (β-arr 1 and β-arr2) coexpressed with or without individual RAMPs. Data are area-under-the-curve (AUC) of the BRET signals for β-arrestin 1/2 recruitment assay. Signals were normalized to the maximum response of GIPR and dose-response curves were analyzed using a three-parameter logistic equation. All data were generated and graphed as means ± SEM of at least three independent experiments, conducted in quadruplicate (cAMP accumulation assay) or duplicate (β-arrestin 1/2 recruitment assay).

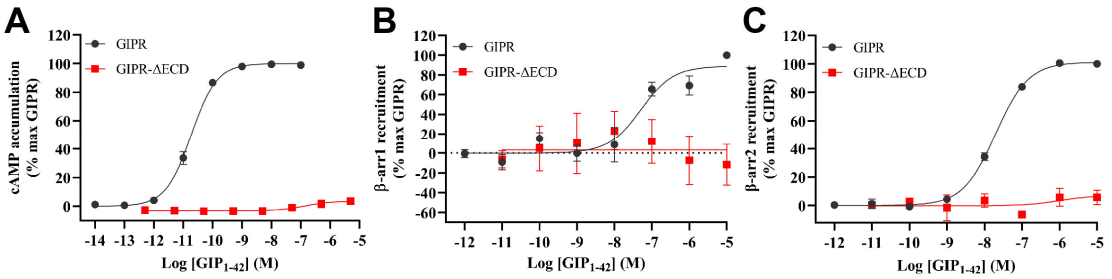

Figure S9. Signaling profiles of GIPR and ECD truncated GIPR (GIPR-ΔECD). (***A***) cAMP accumulation induced by GIP_{1-42} at GIPR or GIPR-ΔECD. The assay was performed in HEK293T cells transiently transfected with constructs of GIPR or GIPR-ΔECD. (***B*** and ***C***) β-arrestin 1/2 recruitment induced by GIP_{1-42} at GIPR or GIPR-ΔECD. HEK293T cells were transiently transfected either with GIPR-Rluc8 and Venus-β-arrestin 1/2 (β-arr1 and β-arr2), or with GIPR-ΔECD-Rluc8 and Venus-β-arrestin 1/2 (β-arr1 and β-arr2). Data are area-under-the-curve (AUC) of the BRET signals. Signals were normalized to the maximum response of GIPR and dose-response curves were analyzed using a three-parameter logistic equation. All data were generated and graphed as means ± SEM of at least three independent experiments, conducted in quadruplicate (cAMP accumulation assay) or duplicate (β-arrestin 1/2 recruitment assay).

Table S1. Category of GIPR SVs and their structural variation.

Category	Name	Length of protein	Transcript ID	NCBI Reference Sequence	Structural variation
Wild-type (WT)	GIPR-205	466	ENST00000590918.6	NP_000155.1	
C terminus variation	GIPR-201	419	ENST00000263281.7		H8 and C terminus variation
	GIPR isoform X5	415		XP_047294557.1	TM7 variation, H8 and C terminus missing
	GIPR-203/ GIPR isoform X9	265	ENST00000585889.1	XP_047294559.1	G265D, 266-466 residues missing
	GIPR isoform X7	291		XP_011525018.1	266-466 residues missing and C terminus variation
	GIPR isoform X8	284		XP_047294558.1	267-466 residues missing and C terminus variation
N terminus variation	GIPR-202 (SV1)	430	ENST00000304207.12	NP_001295347.1	58-93 residues of ECD missing
	GIPR-209 (SV2)	405	ENST00000652180.1		1-93 residues missing and N terminus insertion
Peptide/ Soluble form	GIPR-207	17	ENST00000591322.1		67-83 residues of WT GIPR
Insertions within TM5	GIPR isoform X1	508		XP_011525012.1	TM5 insertion of 42 residues
Insertions within TM5& N terminus/ TM1/TM2/ ECL1 variation	GIPR isoform X2	472		XP_047294555.1	TM5 insertion of 42 residues, 58-93 residues of ECD missing
	GIPR isoform X6	369		XP_011525017.1	TM5 insertion of 42 residues, 1-139 residues (ECD and partial TM1) missing
	GIPR isoform X4	425		XP_011525015.1	TM5 insertion of 42 residues, 129-212 residues (TMs 1, 2 and ECL1) missing

Table S2. Cryo-EM data collection, refinement and validation statistics.

Data collection and processing	SV1–G_s–Nb35 complex	SV2–G_s–Nb35 complex
Magnification	46,685	46,685
Voltage (kV)	300	300
Electron exposure (e^{-}/Å^2)	80	80
Defocus range (μm)	-1.2 to -2.2	-1.2 to -2.2
Pixel size (Å)	1.071	1.071
Symmetry imposed	C1	C1
Initial particle images (no.)	6,613,994	5,853,096
Final particle images (no.)	596,712	463,406
Map resolution (Å)	3.23	3.13
FSC threshold	0.143	0.143
Map resolution range (Å)	2.8–5.5	2.8–5.5
Refinement		
Initial model used (PDB code)	PDB code 7DTY	PDB code 7DTY
Model resolution (Å)	3.23	3.13
FSC threshold	0.5	0.5
Model resolution range (Å)	2.8-5.5	2.8-5.5
Map sharpening B factor (Å^2)	-123.73	-137.14
Model composition		
Non-hydrogen atoms	7,954	7,905
Protein residues	1,035	1,035
Lipids	0	0
B factors (Å^2)		
Protein	127.98	153.34
Ligand	0	0
Lipids	0	0
R.m.s. deviations		
Bond lengths (Å)	0.004	0.004
Bond angles (°)	0.592	0.595
Validation		
MolProbity score	1.78	1.82
Clash score	9.23	9.71
Poor rotamers (%)	0.0	0.0
Ramachandran plot		
Favored (%)	95.88	95.58
Allowed (%)	4.12	4.42
Disallowed (%)	0.0	0.0

Table S3. Summary of the residues with poor cryo-EM density in the structure model.

Model	Category	Protein	Residue
SV1–G_s–Nb35 complex	Side chains were not modeled due to poor cryo-EM densities.	SV1	N88, E89, F91, L92, V103, M104, V107, L125, D155, R156, L158, L211, V212, L225, E246, R253, V256, K257, R264, M269, R290, T291, Q293, M294, R295, R297, D298, L303, V316, H317, F321, T325, E326, E327, Q328, R330, L338, F347, L376, R377
		$G\alpha_s$	E10, R13, K24, Q31, E50, K58, K216, E299, K305, E314, V367, T369
		Gβ	L4, D5, R8, E12, K15, K23, D38, R129, E130, D186, M217, D267, D323
		Gγ	T6, I9, K20, D26, M38, K46
		Nb35	L11, K43, E89
	Residues were not modeled due to poor cryo-EM densities.	SV1	R22-K87, R160-W173
		$G\alpha_s$	M1-K8, R61-T204, S252-N261
		Gβ	M1-S6
		Gγ	M1-N5, E63-L71
SV2–G_s–Nb35 complex	Side chains were not modeled due to poor cryo-EM densities.	SV2	N63, E64, F66, L67, D68, E74, V78, V82, R103, E192, F209, R228, E230, R267, D273, L278, T282, H292, E293, F296, E301, E302, Q303, R305, L313, F322, S328, L330, R344, R352, R353
		$G\alpha_s$	E15, K58, K216, L302, K305, R317, D323, E330, D354, R356, C365, D368, E370
		Gβ	D5, Q6, R8, Q9, E10, E12, K15, D20, K23, D38, R129, D186, E215, D254, D303, D312, D323
		Gγ	I9, Q11, R13, K14, E17, Q18, N24, D26, K29, K32, K46, E47, S57, R62
		Nb35	K43, S54, K76, K87, E89
	Residues were not modeled due to poor cryo-EM densities.	SV2	R135-W148, M1-K62, L355-R360
		$G\alpha_s$	M1-K8, R61-T204, S252-N261
		Gβ	M1-S6
		Gγ	M1-N5, E63-L71

Table S4. Signaling profiles of GIPR, SV1 and SV2 coexpressed with or without individual RAMPs elicited by GIP_{1-42}.

Receptor	cAMP accumulation		β-arrestin 1 recruitment		β-arrestin 2 recruitment	
	pEC_{50} ± SEM	E_{max} ± SEM	pEC_{50} ± SEM	E_{max} ± SEM	pEC_{50} ± SEM	E_{max} ± SEM
GIPR	11.31 ± 0.05	100.00 ± 1.35	8.35 ± 0.15	100.00 ± 5.30	8.14 ± 0.07	100.00 ± 2.35
GIPR+RAMP1	11.09 ± 0.04	99.74 ± 1.12	8.39 ± 0.29	82.64 ± 7.87	8.43 ± 0.14	81.73 ± 3.09**
GIPR+RAMP2	11.31 ± 0.05	100.04 ± 1.44	8.48 ± 0.33	91.08 ± 8.98	8.45 ± 0.10	117.78 ±3.11**
GIPR+RAMP3	9.13 ± 0.06***	96.76 ± 2.38	7.25 ± 0.28*	74.18 ± 8.90	7.36 ± 0.13***	88.17 ± 3.65*
SV1	N.D.	N.D.	N.A.	N.A.	N.A.	N.A.
SV1+RAMP1	N.D.	N.D.	N.A.	N.A.	N.A.	N.A.
SV1+RAMP2	7.53 ± 0.10***	52.49 ± 2.08***	N.A.	N.A.	N.A.	N.A.
SV1+RAMP3	N.D.	N.D.	N.A.	N.A.	N.A.	N.A.
SV2	N.D.	N.D.	N.A.	N.A.	N.A.	N.A.
SV2+RAMP1	N.D.	N.D.	N.A.	N.A.	N.A.	N.A.
SV2+RAMP2	7.58 ± 0.14***	56.34 ± 3.22***	N.A.	N.A.	N.A.	N.A.
SV2+RAMP3	N.D.	N.D.	N.A.	N.A.	N.A.	N.A.

cAMP accumulation and β-arrestin 1/2 recruitment induced by GIP_{1-42} at GIPR, SV1, SV2 as well as that coexpressed with individual RAMPs in HEK293T cells. Signals were normalized to the maximum response of GIPR and dose-response curves were analyzed using a three-parameter logistic equation. All data were generated and graphed as means ± SEM of at least three independent experiments, conducted in quadruplicate (cAMP accumulation assay) or duplicate (β-arrestin 1/2 recruitment assay). One-way ANOVA were used to determine statistical difference (*P<0.05, **P<0.01, ***P<0.001 compared with GIPR). N.A., not active. N.D., values that could not be determined due to incomplete curve fits.

Table S5. Signaling profiles of GIPR and GIPR-ΔECD.

Receptor	cAMP accumulation		β-arrestin 1 recruitment		β-arrestin 2 recruitment	
	pEC_{50} ± SEM	**E_{max} ± SEM**	**pEC_{50} ± SEM**	**E_{max} ± SEM**	**pEC_{50} ± SEM**	**E_{max} ± SEM**
GIPR	10.73 ± 0.03	100.00 ± 0.95	7.30 ± 0.22	89.01 ± 7.19	7.70 ± 0.04	101.19 ± 1.47
GIPR-ΔECD	N.A.	N.A.	N.A.	N.A.	N.A.	N.A.

cAMP accumulation and β-arrestin 1/2 recruitment induced by GIP_{1-42} at GIPR or GIPR-ΔECD in HEK293T cells. Signals were normalized to the maximum response of the GIPR and dose-response curves were analyzed using a three-parameter logistic equation. All data were generated and graphed as means ± SEM of at least three independent experiments, conducted in quadruplicate (cAMP accumulation assay) or duplicate (β-arrestin 1/2 recruitment assay). N.A., not active.